Wave-Number Selection and Traveling Vortex Waves in Spatially Ramped Taylor-Couette Flow

Li Ning, Guenter Ahlers, and David S. Cannell
Department of Physics and Center for Nonlinear Science, University of California, Santa Barbara, California 93106
(Received 16 October 1989)

We report experimental results for wave-number selection in Taylor-vortex flow with slow spatial ramps of the Reynolds number. The accessible range of wave numbers is always much smaller than the Eckhaus-stable range, but the selected wave number depends on the detailed nature of the ramp. For a particular ramp, wave numbers outside the Eckhaus-stable band were selected, leading to a periodic state of traveling vortices. The selected wave numbers and the frequencies of the periodic state agree well with a phase-dynamical calculation by Riecke and Paap.

PACS numbers: 47.20.−k, 05.70.Ln

In extended homogeneous dissipative systems, spatially varying patterns usually grow out of a uniform background when an external control parameter exceeds some threshold value. The pattern selection involved in this process has attracted much theoretical and experimental attention in recent years.[1] The stable ranges of the patterns are generally restricted by bulk instabilities which limit their characteristic wave numbers to bands of finite width. Within these bands, however, nonuniqueness is a characteristic feature of nonlinear systems. An interesting question which arises is whether particular circumstances may prevail which lead to the selection of a specific pattern from among those which are within the stable band.

We will restrict ourselves here to the particularly simple case of one-dimensional patterns, where the interesting spatial variation takes place only in one physical direction. In that case, it was predicted by Kramer *et al.*[2] and observed experimentally by Dominguez-Lerma and co-workers[3,4] that a spatial variation of the control parameter R (which determines the strength of the external driving) from below to above its threshold value resulted in a unique pattern. However, the particular pattern chosen depends upon the details of how R varies from its threshold value to its bulk value in the interior of the system.[2,5] Recently, Riecke and Paap[6] have predicted that it is possible to construct particular cases where the variation of R leads to the selection of a wave number which lies *outside* the band of stable states for the homogeneous system. We report here on experiments which correspond to such a case. We find that the selection of an unstable state can indeed be achieved, and that its selection leads to periodic transitions in the homogeneous section of the system. In our case, these transitions occur because the vortices in the straight section have been compressed beyond the Eckhaus-stable range, and each transition results in the loss of one wavelength of the pattern. This loss is periodically replenished, however, by a traveling wave (TW) moving in the section of varying R and towards the homogeneous part. Thus, a *dynamic* state is created by the selection of an *unstable* state. We have measured the selected wave numbers and TW frequencies, and find them to be in quantitative agreement with the predictions.[6] This agreement is a rather spectacular success of the phase-dynamical methods[7,8] which were used in the calculations.

The phenomenon studied by us differs qualitatively from the one first suggested by Kramer *et al.*,[2] and investigated by Rehberg *et al.*,[9] where two different ramps selected different *stable* wave numbers at the two ends of a straight section. In that case the consequent wave-number gradient produced a traveling wave from one ramp to the other through the homogeneous part of the system, and no instability mechanism was involved.

The system we investigated was Taylor-vortex flow[10] (TVF) between two concentric cylinders, with the inner one rotating. The cylinders had constant radii $r_0^{i,o}$ for axial positions $z>0$ with $r_0^i/r_0^o=0.745$ cm. Here the superscripts i and o stand for the inner and outer cylinders, respectively. This straight, or homogeneous, section had a gap $d_0=r_0^o-r_0^i=0.639$ cm and was terminated at $z=L_h d_0$ by a rigid, nonrotating collar, which essentially filled the gap for $z>L_h d_0$. For $z<0$, the radii varied as $r^{i,o}=r_0^{i,o}+\alpha^{i,o}z$, giving a spatial ramp for the gap $d(z)=d_0+(\alpha^o-\alpha^i)z$. At $z=-L_r d_0$, the system was terminated by another nonrotating collar. For negative z, the variation of the radii leads to a variation of the control parameter (Reynolds number) with z. Thus, for appropriate $\alpha^{i,o}$ it is possible to have $\epsilon(z)\equiv R(z)/R_c(z)-1=\epsilon_0>0$ in the homogeneous section, with $\epsilon(z)<0$ at $z=-L_r d_0$. When $\alpha^{i,o}$ are vanishingly small, this condition is predicted[2,6] to lead to the selection of a unique wavelength λ_0 of the vortex pairs in the straight section, with λ_0 dependent upon α^o/α^i and ϵ_0. For finite but small $\alpha^{i,o}$ a unique state is still selected, but λ_0 depends nearly periodically upon L_h, and its extrema define a small band which can, in practice, be much more narrow than the band of stable states.[3,4,11,12]

Most of our measurements were for $\alpha^i=0.0074$ rad

and $\alpha^o = 0.0151$ rad, corresponding to both cylinder diameters decreasing as z becomes more negative. We will refer to this system as ramp 1. It had lengths L_h variable from 10 to 24, and $L_r = 33.3$, and led to the selection of a time-periodic state for $\epsilon_0 \gtrsim 0.2$. More limited measurements were also made for a second ramp, which has $\alpha^i = -0.0075$ rad, $\alpha^o = 0$, and selected stable time-independent states for our range of ϵ_0. The temperature of the apparatus was held constant to $\pm 0.01\,^\circ$C. The fluid was 40% by volume glycerol and 60% water. Most of the results reported here were obtained with flow visualization obtained by adding 1 vol% of a Kalliroscope suspension of polymeric flakes.[13] Our main results were confirmed, however, by laser-Doppler velocity measurements. Wavelengths were determined with a traveling microscope. Digitized Kalliroscope flow-visualization contours in the axial direction were obtained with a computer-interfaced video camera. A contour plot, consisting of a time sequence of such contours each plotted with a vertical displacement relative to the previous one, provides a good visualization of the dynamics of the selected time-periodic state.

In Fig. 1 we show (solid circles) one-half the wavelength $\lambda(z)$ [width of a vortex pair normalized by the local gap $d(z)$] together with individual vortex widths (open circles) measured for ramp 1 as a function of position z. Also shown in the figure is $\epsilon(z)$. In the region where $\epsilon < 0$, vortices were not observable. Near $z = -15 d_0$, ϵ passes through zero. At that location, $\lambda(z)$ has a value close to 2.0, the critical value at the onset of TVF. As z and ϵ increase, $\lambda(z)$ decreases until $z = 0$ is reached, after which it remains constant in the homogeneous section. We believe the alternating vortex widths in the ramp are the result of a large-scale flow[11] induced by the ramp. Such a flow would tend to alternately increase and decrease the amplitudes of individual vortices. This effect has been observed before by Wimmer[14,15] for flow between concentric cones. As can be seen, this effect persists for some distance into the homogeneous section.

In Fig. 2, we show the experimental results for the wave numbers $q = 2\pi d_0/\lambda$ in the homogeneous section for both of our ramps. Each horizontal bar represents the range of q which was observable as L_h was varied quasistatically. The data at large q are for ramp 1, and those at small q correspond to ramp 2. The dashed lines through the data are the predictions of Riecke and Paap.[6] The data for ramp 2 remain in the stable band of states, the limit of which is given by the Eckhaus instability[4,16,17] shown by the solid curve.[18] The wave numbers selected by ramp 1, however, reach the Eckhaus boundary at large q for $\epsilon_0 \simeq 0.2$. Below this value of ϵ_0, a time-independent state was selected. Since the wavelength in the homogeneous section varied by about 2% for $\epsilon \gtrsim 0.15$, and this corresponds to about 7% uncertainty in $q/q_c - 1$, we regard the agreement with the theory as reasonably satisfactory.

The behavior of ramp 1 for $\epsilon_0 \gtrsim 0.2$ is illustrated by the contour plots shown in Figs. 3 and 4. The region of negative z contained a TW of vortices moving up the ramp toward the homogeneous section. The vortices in the homogeneous part were continually compressed by the incoming vortices, driving them beyond the Eckhaus-stable range. The loss of a vortex pair occurred periodically. Although not apparent from the contour plots, visual observation showed that the pattern retained its cylindrical symmetry throughout the cycle, as would be expected for the Eckhaus mechanism. In the case shown in Fig. 3, the vortex-pair loss occurred near $z = 2d_0$; but for values of ϵ closer to 0.2, as in Fig. 4, the

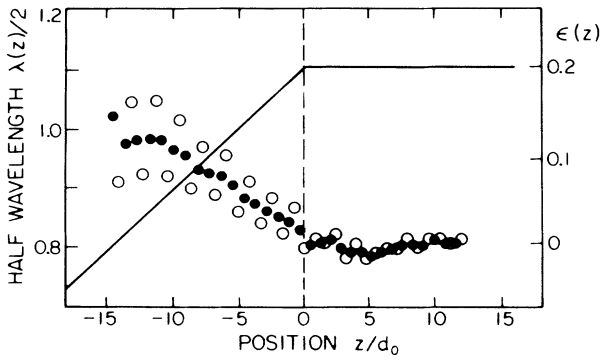

FIG. 1. Individual vortex widths (open circles) and their pairwise averages (solid circles), normalized by the local gap $d(z)$, as a function of axial position z for TVF in a spatially ramped geometry. The solid line gives the value of $\epsilon(z) = R(z)/R_c(z) - 1$, with positive z corresponding to the homogeneous section of the apparatus.

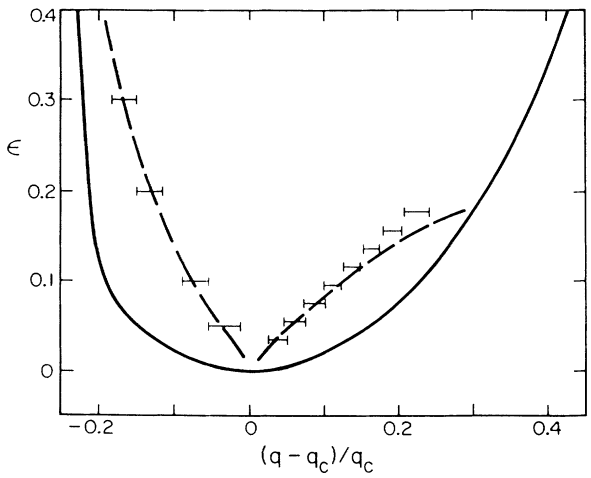

FIG. 2. Range of experimentally observed wave numbers (horizontal bars), as a function of ϵ, for two different spatial ramps. The dashed lines are the theoretical predictions for the limiting case of infinitesimal ramp angles. The solid line gives the location of the Eckhaus instability, which limits the band of stable states.

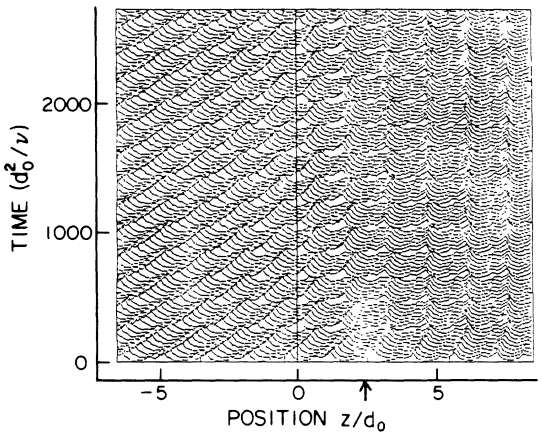

FIG. 3. Contour plot for ramp 1 with $\epsilon_0=0.30$. The traveling wave of vortex pairs in the ramped section is apparent. Vortex pairs are lost periodically in time near the location indicated by the arrow at the abscissa. The early part of this figure (time $\lesssim 200$) is a transient which resulted from changing ϵ_0.

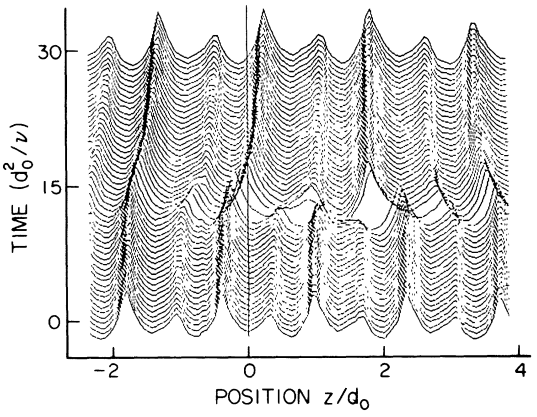

FIG. 5. Details of the vortex-pair-loss process in time (arbitrary origin) and space under the same conditions as Fig. 3.

TW had a smaller speed, and the loss occurred deeper in the interior of the homogeneous section near the arrow at $z=7d_0$. The details of the vortex-pair-loss mechanism for the conditions of Fig. 3 are illustrated in Fig. 5.

In Fig. 6 we show the dimensionless angular frequency ω of the signal observed at a fixed position near $z=0$ as a function of ϵ_0 (here time is scaled by $d_0^2/\nu=10.8$ sec, where ν is the kinematic viscosity of the fluid). For $\epsilon_0\gtrsim 0.2$, where the system selects an unstable wave number, ω increases from zero with increasing ϵ_0. Near $\epsilon_0=0.5$, however, ω reaches a maximum. For larger ϵ_0, ϵ is positive throughout this system, and the entire length L_r of the ramp is filled with vortices. In that case the value of q at $z=-L_r d_0$ can be less than q_c, and a wider range of stable states becomes available to accommodate more of the variation of q that is required[6] in the ramp section. The result is a decreasing TW frequency with further increase in ϵ_0. For $\epsilon_0\gtrsim 0.8$, ω is zero once again because beyond this point the entire required variation of q along the ramp[6] can be accommodated within the Eckhaus-stable band.

The solid and dashed lines in Fig. 6 are the frequencies predicted by Riecke and Paap[6,19] for $\alpha^i/\alpha^o=0.49$ and 0.53, respectively (our apparatus had $\alpha^i/\alpha^o=0.49\pm 0.03$). As can be seen, the prediction is quite sensitive to the ratio of the ramp angles. In addition, in the experimental system with nonzero $\alpha^{i,o}$, the precise value of ϵ_0 where a TW can first be observed depends slightly upon L_h, because L_h determines which wave number within the small band represented by the horizontal bars in Fig. 2 is chosen when the Eckhaus boundary is crossed. A third complication is that the theory

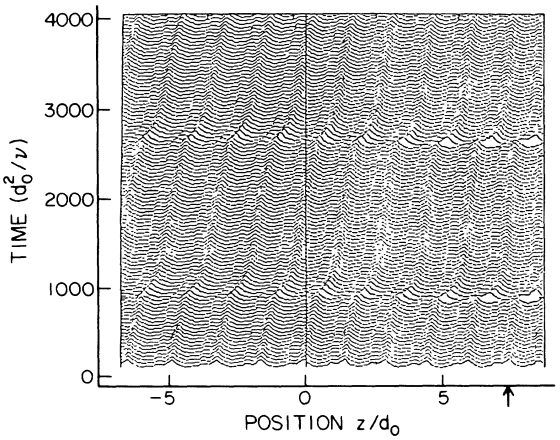

FIG. 4. Contour plot as in Fig. 3, but for $\epsilon_0\simeq 0.20$.

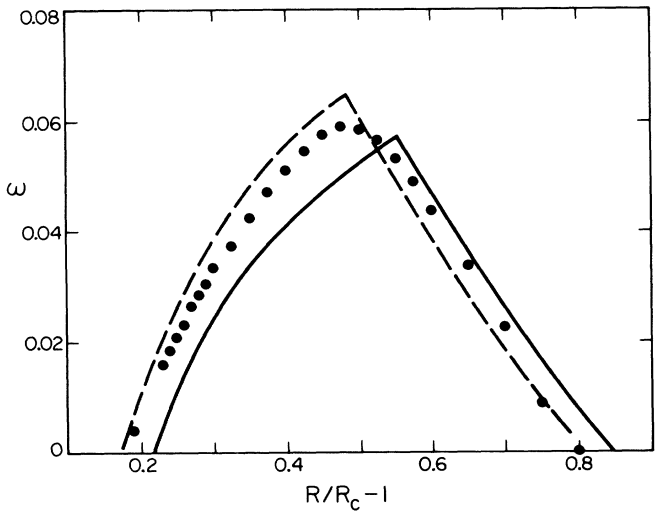

FIG. 6. Traveling-wave frequency as a function of ϵ_0 for one aspect ratio ($L_h=18.0$). The solid circles represent our measurements. The solid line is the prediction for $\alpha^i/\alpha^o=0.49$, while the dashed line is for $\alpha^i/\alpha^o=0.53$ (our apparatus had $\alpha^i/\alpha^o=0.49$).

neglects the formation of an Ekman vortex near $z=-L_r d_0$ when $\epsilon>0$ throughout the system (presumably this vortex would change the effective length of the ramped portion of the system). Finally, the theory models the actual loss of a vortex pair in the interior of the straight section by means of a boundary condition at the point where the ramp and the homogeneous section join. This condition corresponds to assuming that the Eckhaus mechanism in the interior of the straight section maintains a constant wave number at the ramp end equal to that of the Eckhaus boundary at $\epsilon=\epsilon_0$. In view of these minor complications we regard the agreement as very good indeed.

In this Letter we have presented experimental results which confirm the theoretical prediction[6] that unstable states can be selected in nonequilibrium systems by appropriate spatial variation of the control parameter. When such a state is selected in TVF, the instability mechanism leads to a time-periodic state consisting of a traveling wave of vortices in the ramped section and a periodic vortex-pair loss in the homogeneous section. Although traveling waves have been created previously in Rayleigh-Bénard convection by the selection of different wave numbers at the two ends of a homogeneous section,[9] their creation by the selection of an unstable state has, to our knowledge, not been observed before. Our measurements of the selected wave numbers and of the traveling-wave frequencies agree quantitatively with calculations by Riecke and Paap[6] based on a phase-dynamical approach.

We are grateful to H. Riecke for numerous helpful discussions, and for providing us with the theoretical results in Fig. 6 prior to publication. This work was supported by the National Science Foundation through Grant No. DMR88-14485.

[1]See, for instance, *Cellular Structures in Instabilities,* edited by J. E. Wesfreid and S. Zaleski (Springer-Verlag, New York, 1984); *Spatio-Temporal Coherence and Chaos in Physical Systems,* edited by A. R. Bishop, G. Grüner, and B. Nicolaenko (North-Holland, Amsterdam, 1986).

[2]L. Kramer, E. Ben-Jacob, H. Brand, and M. C. Cross, Phys. Rev. Lett. **49**, 1891 (1982).

[3]D. S. Cannell, M. A. Dominguez-Lerma, and G. Ahlers, Phys. Rev. Lett. **50**, 1365 (1983).

[4]M. A. Dominguez-Lerma, D. S. Cannell, and G. Ahlers, Phys. Rev. A **34**, 4956 (1986).

[5]L. Kramer and H. Riecke, Z. Phys. B **59**, 245 (1985).

[6]H. Riecke and H. G. Paap, Phys. Rev. Lett. **59**, 2570 (1987).

[7]Y. Pomeau and P. Manneville, J. Phys. (Paris), Lett. **40**, 610 (1979).

[8]H. R. Brand, in *Propagation in Systems far from Equilibrium,* edited by J. E. Wesfreid, H. R. Brand, P. Manneville, G. Albinet, and N. Boccara (Springer-Verlag, Berlin, 1988), p. 206.

[9]I. Rehberg, E. Bodenschatz, B. Winkler, and F. H. Busse, Phys. Rev. Lett. **59**, 282 (1987).

[10]G. I. Taylor, Philos. Trans. Roy. Soc. London A **223**, 289 (1923).

[11]M. C. Cross, Phys. Rev. A **29**, 391 (1984).

[12]H. Riecke, Phys. Rev. A **37**, 636 (1988).

[13]Kalliroscope Corporation, P.O. Box 60, Groten, MA 01450, rheoscopic liquid AQ-1000; see also P. Matisse and M. Gorman, Phys. Fluids **27**, 759 (1984).

[14]M. Wimmer, Z. Angew. Math. Mech. **63**, T299 (1983).

[15]M. Wimmer, Z. Angew. Math. Mech. **65**, T255 (1985).

[16]W. Eckhaus, *Studies in Nonlinear Stability Theory* (Springer-Verlag, New York, 1965).

[17]S. Kogelman and R. C. DiPrima, Phys. Fluids **13**, 1 (1970).

[18]H. Riecke and H. G. Paap, Phys. Rev. A **33**, 547 (1986).

[19]H. Riecke and H. G. Paap (private communication).